1·0 2·8 2·5
5·0 3·15 2·2
5·6
6·3 3·5
1·1 4·0 2·0
4·5 1·8
1·25 1·4 1·6

NATIONAL BUREAU OF STANDARDS
MICROCOPY RESOLUTION TEST CHART

AFAL-TR-77-33

MAGNETIC LPE CRYSTALLINE FILMS
FOR SMALL BUBBLE DIAMETER
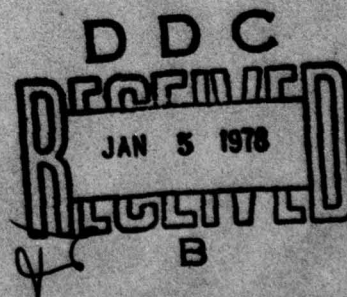CYLINDRICAL-DOMAIN MEMORY APPLICATIONS

Sperry Research Center
100 North Road
Sudbury, Massachusetts 01776

July 1977

Technical Report AFAL-TR-77-33
Interim Report for Period June — December 1976

AIR FORCE AVIONICS LABORATORY
AIR FORCE WRIGHT AERONAUTICAL LABORATORIES
AIR FORCE SYSTEMS COMMAND
WRIGHT-PATTERSON AIR FORCE BASE, OHIO 45433

DDC
RECEIVED
JAN 5 1978
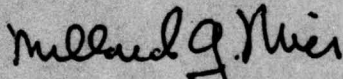B

REPORT DOCUMENTATION PAGE	READ INSTRUCTIONS BEFORE COMPLETING FORM

1. REPORT NUMBER	2. GOVT ACCESSION NO.	3. RECIPIENT'S CATALOG NUMBER
AFAL-TR-77-33		

4. TITLE (and Subtitle)	5. TYPE OF REPORT & PERIOD COVERED
MAGNETIC LPE CRYSTALLINE FILMS FOR SMALL BUBBLE DIAMETER CYLINDRICAL-DOMAIN MEMORY APPLICATIONS.	Interim Report. June — December 1976,
	6. PERFORMING ORG. REPORT NUMBER
	SCRC-CR-77-1

7. AUTHOR(s)	8. CONTRACT OR GRANT NUMBER(s)
M. Kestigian, W. R. Bekebrede and A. B. Smith	F44620-76-C-0121

9. PERFORMING ORGANIZATION NAME AND ADDRESS	10. PROGRAM ELEMENT, PROJECT, TASK AREA & WORK UNIT NUMBERS
Sperry Research Center 100 North Road Sudbury, MA 01776	

11. CONTROLLING OFFICE NAME AND ADDRESS	12. REPORT DATE
Air Force Avionics Laboratory Air Force Wright Aeronautical Laboratories Air Force Systems Command Wright Patterson, AFB, Ohio 45433	July 1977
	13. NUMBER OF PAGES
	35

14. MONITORING AGENCY NAME & ADDRESS(if different from Controlling Office)	15. SECURITY CLASS. (of this report)
34p.	Unclassified
	15a. DECLASSIFICATION/DOWNGRADING SCHEDULE

16. DISTRIBUTION STATEMENT (of this Report)

Approved for public release; distribution unlimited.

DDC RECEIVED JAN 5 1978 B

17. DISTRIBUTION STATEMENT (of the abstract entered in Block 20, if different from Report)

18. SUPPLEMENTARY NOTES

19. KEY WORDS (Continue on reverse side if necessary and identify by block number)

Stripe Width	Garnet
Bubble Collapse Field	$(LaEuTm)_3(FeGa)_5O_{12}$
Bubble Memory Devices	$(SmTm)_3(FeGa)_5O_{12}$
Liquid Phase Epitaxy	$(TbTm)_3(FeGa)_5O_{12}$
Crystalline Films	2 micron

20. ABSTRACT (Continue on reverse side if necessary and identify by block number)

This was an interim technical report which covers the research performed during the first six months of the contract period. The report includes a description of the preparation, characterization and magnetic property evaluation of liquid-phase epitaxial (LPE) crystalline-garnet films for $2 \mu m$ bubble diameter memory devices. Over four-hundred and fifty different LPE preparations were made and thin films grown. Representative results of this research were presented in tabular form. Magnetic measurements included, in addition to the usual experiments, temperature dependence data.

(Continued on reverse side)

DD FORM 1 JAN 73 1473 EDITION OF 1 NOV 65 IS OBSOLETE

408 199

20. ABSTRACT

Of the many garnet compositions investigated, lanthanum europium thulium gallium iron garnet and samarium thulium gallium iron garnet exhibited percentage changes over the $-55°$ to $+125°$ C temperature range which are well within the contract specified limits. The q for these films was found to be 5 to 6, as compared to the design goal minimum value of 3. Therefore, since all static small bubble diameter properties of these two LPE film compositions more than meet the contract objectives, the program will proceed with the measurement of their dynamic magnetic properties.

PREFACE

This project was initiated by the Air Force Office of Scientific Research (AFSC), United States Air Force under the direction of Dr. Millard Mier (AFAL/DHE). This is the Interim Technical Report for the period June 1976 through December 1976.

The research described was carried out at the Sperry Research Center, Sudbury, Massachusetts 01776. The project manager at SCRC is M. Kestigian.

TABLE OF CONTENTS

v

SECTION I

OBJECTIVES

This research is concerned with the preparation, characterization and
evaluation of crystalline garnet magnetic films. The liquid-phase epitaxial
growth technique was used to deposit magnetic thin films on commercial non-
magnetic 3G substrates. These thin films were evaluated for use in small
bubble diameter cylindrical domain memory devices. Research performed in
addition to formulation and thin film deposition studies included measurement
of wall energy, anisotropy, temperature coefficient, temperature range and
magnetization. Analyses involved the presence of impurities, nonstoichiom-
etry and charge compensation considerations. The goal is to prepare and
evaluate a small bubble diameter (less than 2 μm) LPE crystalline garnet film
with the following characteristics:

wall energy density   0.25 ergs/cm^2

$q = Hk/4\pi M_s > 3$

velocity $>$ 1000 cm/sec @ $\Delta H = 5$ Oe

temperature coefficient   .2 %/$^{\circ}$C

rotating field drive at 10^6 bit/sec shift rate $<$ 25 Oe

1

SECTION II

SPERRY RESEARCH CENTER TECHNICAL APPROACH

The overall technical approach to be used in the development of a
small-bubble diameter cylindrical-domain mass-memory material emphasizes
the formulation, preparation, characterization, evaluation and testing of
magnetic crystalline thin films.

The rare earth iron garnet magnetic thin films have been found to be
the most promising 3 to 8 μm bubble diameter materials for bubble memory
devices. Large cross sectional area films of suitable perfection and de-
sirable magnetic properties have been obtained from liquid-phase epitaxial
deposition experiments. It is reasonable to assume that these successes can
be extended to include small bubble diameter garnet compositions.

Gadolinium gallium garnet (3G) has found widespread use as the non-
magnetic substrate material for the LPE deposition of magnetic garnet thin
films. No doubt research extended to include 1 to 2 μm bubble diameter
materials will also utilize 3G substrates. Since polished 3G substrate
slices of adequate quality are readily available commercially, gadolinium
gallium garnet boules will not be grown. However, if for any reason com-
mercial substrate sources are not adequate for the deposition of small
bubble diameter thin films, nonmagnetic garnet single crystals will be grown
from the direct melt by the Czochralski technique, oriented crystallo-
graphically, cut, polished and cleaned prior to use.

The approach to be followed in the growth of magnetic crystalline
films will be the liquid-phase epitaxial method. This technique has proven
to be the superior method for obtaining high perfection magnetic films.
While both tipping and dipping modifications of LPE growth have been employed,
the horizontal wafer dipping reverse rotation process will be used for the
growth of small bubble diameter crystalline thin films.

The selection of the optimum small bubble diameter crystalline garnet
composition will take into consideration the results of several fundamental

2

magnetic property measurements. Dynamic conversion, hard bubble suppression, propagation angle, mobility, coercivity, temperature dependence of magnetic properties, and anisotropy are parameters that must be investigated and understood. These experiments must be supplemented by magnetization, bubble diameter and bubble collapse measurements on all samples.

Compositions to be grown and evaluated include europium thulium gallium iron garnet and europium thulium calcium germanium iron garnet. Investigations will be conducted with the objective of preparing a rare earth iron garnet composition which concentrates all of the transition metal nonmagnetic cations exclusively in the tetrahedral site. The use of germanium instead of gallium approaches this condition. Another approach that might prove to be superior would be to use vanadium, together with a monovalent cation for charge and cation compensation.

SECTION III

SUMMARY

Rare-earth iron garnet compositions were formulated, films deposited by liquid-phase epitaxy, and magnetic evaluation measurements performed. The results of pertinent magnetic property experiments were used to select improved rare-earth iron garnet compositions for small bubble diameter magnetic memory applications. Representative results of this research are given in tabular form in Appendix I. Temperature dependence data were obtained for a number of small bubble diameter rare-earth iron garnet thin films deposited on 3G [111] polished substrates. Of these garnets, two compositions $\left[(LaEuTm)_3(FeGa)_5O_{12} \text{ and } (SmTm)_3(FeGa)_5O_{12}\right]$ exhibit percentage changes over the -55 to +125 temperature range which are well within the specified limits. The q for these films was found to be 5 to 6, as compared to a q $>$ 3 design goal. In fact, all of the static small bubble diameter properties of these two materials more than adequately meet the contract objectives. The evaluation of their dynamic magnetic properties will be undertaken during the coming months of the contract.

4

SECTION IV

SUBSTRATE PREPARATION AND CHARACTERIZATION

Gadolinium gallium garnet (3G) substrates have been obtained as polished wafers from Allied Chemical Company. The specifications under which these wafers were purchased are as follows:

Diameter = 1 inch

Thickness = 0.020 inch

Flat to 3 fringes over central 85% of area

Core, birefringence, and inclusion free

Crystallographically oriented to within 0.5 degree of [111].

Five or fewer defects over central 85% of area, as revealed by a 2-minute etch in 220° C phosphoric acid, using Nomarski interference contrast microscope.

Until recently, Allied has been able to promptly supply wafers meeting the above specifications. However, long delays were experienced on the last order placed with them, and a partial shipment received in September had to be returned as unacceptable because of an excessive number of defects and inclusions. We suspected that the difficulty was caused by their recent move of the 3G production facility to Charlotte, North Carolina. Discussions with Allied over the past three months tended to confirm these suspicions. Finally, on December 15, a visit was made to Charlotte by M. Kestigian and B. Stein (Univac, Blue Bell, Pa.) to review the situation with them.

Each 3G wafer, immediately prior to being used as an epitaxial substrate, is cleaned by the following sequence of steps:

1. Rinse in acetone
2. Rinse in demineralized water
3. Boil in trichloroethylene for $\frac{1}{2}$ hour
4. Boil in 10% sodium hydroxide for $\frac{1}{2}$ hour
5. Rinse in demineralized water
6. Immerse in phosphoric acid at 120°C for 1 minute
7. Rinse in hot tap water

8. Rinse in demineralized water

9. Blow dry with filtered air gun.

SECTION V

LIQUID-PHASE EPITAXIAL FILM DEPOSITION

The basic liquid-phase epitaxy (LPE) growth procedure used throughout this contract period is conventional for bubble memory films and utilizes horizontal dipping of [111] crystallographically oriented $Gd_3Ga_5O_{12}$ (3G) polished substrates.

The substrate is cleaned prior to use and is supported by a three-pronged platinum wire holder. A lowering-rotation mechanism is used to position the substrate above the solution for pre-heat purposes until temperature equilibrium is reached. Excessive exposure to the vapors above the solution causes defects to form, whereas insufficient heating results in uncontrolled film deposition. The growth process must be carried out under isothermal conditions. Any temperature fluctuations during the growth process produce pronounced film property differences.

Kanthal wound-electrically heated-resistance furnaces were used in the LPE experiments. The temperature profile in a single zone furnace is determined largely by furnace geometry, conduction losses from the furnace ends and by the position of baffles which minimize convection currents. A zone uniform in temperature to $\pm 1^o$ was 8 cm in length and decreased by 2° one half inch above the solution surface.

Garnet films were grown on [111] 3G substrates by LPE techniques previously described by numerous researchers. During this study, the substrates were rotated-reverse rotated with a 2-second period at a rate of 60 rpm. Rotation rates less than 30 rpm and greater than 100 rpm led to a degradation of thickness uniformity. A 600 rpm rotation was used when the grown film was withdrawn from the solution. This procedure resulted in obtaining higher quality magnetic films, as any flux residue that had adhered to the film was removed quickly by this procedure.

Succeeding LPE film growth experiments were carried out after immediate magnetic property measurements were performed. These characterization

studies included lattice-match-mismatch, film thickness, bubble diameter, magnetization, ℓ , q , and anisotropy measurements. Adjustment in solution composition, deposition procedure and deposition conditions were made on the basis of these evaluation measurements. We realize these evaluation studies do not include dynamic properties; however, unless a film composition exhibits the desired static magnetic properties, it will not meet contract objectives. What this preliminary evaluation procedure does accomplish is that sufficient results are obtained to direct succeeding film growth studies with a minimum of lapsed time.

Saturation temperature T_S was defined for each solution as the temperature at which the growth rate was just discernible (less than 0.05 μm/ min for a minimum growth time of 10 minutes. Film deposition was carried out 10 to 20° below the observed saturation temperature for any given solution.

Distribution coefficients employed during this phase of the program were controlled such that the garnet phase was the stable species in any growth process, regardless of film deposition or solution composition modifications. A listing of all R values and/or adjustments would serve no meaningful purpose and is omitted to conserve space and to yield a simpler, more managable report.

During the course of this contract, over 250 LPE film depositions have been made in the search for an improved small bubble diameter crystalline composition. A typical melt composition for the LPE growth of $(LaEuTm)_3 (GaFe)_5 O_{12}$ garnet films in mole per cent is as follows:

La_2O_3	0.044
Eu_2O_3	0.21
Tm_2O_3	0.56
Ga_2O_3	0.63
Fe_2O_3	8.86
PbO	84.40
B_2O_3	5.10

8

This preparation yields films with less than two micrometer bubble diameter at a growth rate of approximately 0.9 μm/minute.

MAGNETIC FILM EVALUATION TECHNIQUES

The magnetic characterization of a bubble material involves the measurement of a variety of parameters. Perhaps the most fundamental of these measurements is the determination of magnetization, $4\pi M$, and wall energy, σ_w, since all the static bubble properties can be deduced from these two parameters. Alternatively, one can express the static bubble properties in terms of $4\pi M$ and the characteristic length ℓ, which is related to σ_w and $4\pi M$ according to the familiar relationship

$$\ell = \frac{\sigma_w}{4\pi M^2}$$

To determine these basic parameters, we use the Fowlis-Copeland technique[1,2] in which one measures the stripe width and bubble collapse field. The $4\pi M$, σ_w, and ℓ can readily be calculated from these results using the formulas given in references 1 and 2.

As with room-temperature measurements, the temperature dependence of $4\pi M$ and ℓ can also be obtained using the Fowlis-Copeland technique. In obtaining the results presented below, the sample temperature was controlled with a specially constructed hot stage in which a controlled flow of nitrogen gas was used to obtain both hot and cold temperatures. The gas was heated by an electric heater or cooled by passing through a copper tube immersed in liquid nitrogen. No heater was incorporated in the sample chamber itself because such heaters (unless very specially wound) generate magnetic fields that would interfere with the measurement. The sample chamber was designed so that the hot (or cold) gas does not pass directly over the sample; instead, it heats (or cools) the closed chamber in which the sample resides. This arrangement insures that the sample temperature is the same as that of the metal sample chamber which can readily be monitored with a thermocouple. The required observations of the domains during these measurements were made using a polarizing microscope which was conventional except for the method used to determine stripe width. A

Vickers binocular shearing eyepiece (Bausch and Lomb 31-76-28) was used for this measurement, thereby achieving a precision which would have been impossible with conventional filar micrometer eyepieces.

In addition to employing this precise measuring device, several other precautions are necessary to avoid an appreciable amount of scatter in the stripe width measurements. This scatter will occur unless the stripe domains are relatively straight over a distance that is at least ten times their width. However, this is not the configuration that the domains normally adopt after the application of either a dc or an ac field perpendicular to the sample. To obtain the desired long, straight domains, we apply an in-plane ac field[2]. We also rotate the sample to find the orientation which gives the straightest stripes. This procedure is required because the stripes have obvious preferred directions reflecting the symmetry of the [111] orientation of the sample. A relatively large in-plane field is required for this initial straightening procedure; then before each measurement, a smaller field is used which is just sufficient to cause a noticeable vibration of the domain walls. This motion insures that the coercivity is overcome so that the domains can assume their equilibrium width at each new temperature. The in-plane field is generated by passing up to ~5A at 60 Hz through a pair of 100-turn rectangular Helmholtz coils having inside dimensions of ~ 4 x 14 cm.

In order to obtain bubble collapse field data, it is necessary to generate new bubbles at each measuring temperature. To avoid the necessity for opening the stage to cut stripes into bubbles, we have installed a small coil inside the sample chamber under the sample. This is a two-layer pancake coil wound with 15 turns of No. 30 wire on a 6.5 mm o.d. nylon form 0.9 mm thick. Using a pulse generator of 10A maximum output and ~ 0.015 μ-sec rise time, a combination of pulse width and bias field which will cut stripes into bubbles is determined experimentally for each new sample. It is true that these pulses may generate some hard bubbles. However, in experiments on these and many other materials, we have found that some normal bubbles are _always_ generated also. Our results are not affected

11

by the hard bubbles, since we read the collapse field of the _first_ bubble to collapse and this must be one of the normal bubbles.

In addition to measurements of ℓ and $4\pi M$, we have also made room-temperature measurements of the anisotropy constant K_u. This is one of the most important bubble material parameters, since it determines bubble stability and influences ℓ according to the relation

$$\ell = \frac{\sqrt{AK_u}}{\pi M^2} \qquad (1)$$

(where A is the exchange constant). In our measurements of K_u, we have used the Kurtzig-Hagedorn method[3,4,5] in which one observes the magnitude of in-plane field required to extinguish the stripe domains observed via the Faraday effect. The details of the experimental procedure for making this measurement may be found in reference 4. The magnitude of K_u is determined from these experiments by using the method described by Druyvesteyn et al[6].

An important auxilliary parameter that can be calculated from the basic material parameters is the bubble stability factor q. This parameter is the ratio between the anisotropy field and the magnetization. Since the anisotropy field is equal to $2K_u/M$, the q is given by

$$q = \frac{K_u}{2\pi M^2} . \qquad (2)$$

Because of the importance of this parameter to bubble device applications, we will frequently give this parameter in addition to K_u, ℓ, and $4\pi M$.

SECTION VII

MAGNETIC FILM EVALUATION RESULTS

A. Magnetic Film Processing Procedures

The as-grown LPE film is immediately cleaned in nitric acid to remove any excess flux which has adhered to it upon withdrawal from the melt. It is then rinsed in demineralized water and blown dry, after which it is ready for characterization.

The film is first examined for the presence of defects on a Leitz metallurgical microscope equipped with Nomarski interference contrast. In general, defects arise in two ways: 1) by propagation from the surface of the substrate, and 2) by incorporation during growth from precipitates or other foreign bodies in the melt. Good quality, clean, properly handled substrates essentially eliminate the propagated variety. The others are controlled by careful preparation of the melt and proper temperature control to insure that precipitation does not occur.

B. Film Thickness Measurements

Epitaxial film thicknesses were measured by optical interference on a Leitz metallograph fitted with a Bausch & Lomb grating monochrometer. The film thickness at any point on the wafer can be calculated by measuring the wavelength change required to cause the fringe system to move an integral number of fringe widths. In addition, the static fringe pattern, i.e., at a fixed wavelength, shows at a glance how uniform the film thickness is. The LPE films delivered under the subject contract have been flat to within one fringe (about 0.1 μm) over the central 85% of the area. There are unavoidable thickness variations in the immediate vicinity of the contact points where the substrate is held in its platinum holder during film growth.

C. Film-Substrate Lattice Parameter Measurements

The relative lattice parameter of the LPE film, i.e., how well it matches that of the substrate, is measured by x-ray diffraction, using a Philips wide-angle goniometer and copper Kα radiation. The film and sub-

13

strate (888) reflections are recorded and their angular difference is a
measure of Δa , the film/substrate mismatch. Precision is enhanced by the
use of a very narrow (1/12°) divergence slit and the smallest goniometer
speed (1/8°/minute). The lowest value of Δa measurable by this technique
is about 0.005Å, below which the film and substrate reflections are not
resolved. All films delivered thus far had Δa values < 0.005Å.

D. **Magnetic-Film Property Measurements**

Before presenting the results of our measurements of small-
bubble garnets, a brief introduction is necessary to put these results in
perspective. A general formula for the bubble garnet materials we have
grown is:

$$(R' \quad R'' \quad R''' \quad ....)_3 \quad Fe_{5-x}N_x \quad O_{12}$$
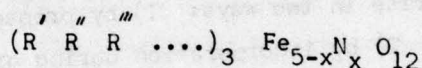
where: R_1, R_2, etc. are rare earths (or yttrium or calcium)

N is a non-magnetic ion, such as Ga or Ge.

The fundamental properties of a garnet, such as the uniaxial anisotropy
constant and the inherent damping of the wall motion, are determined almost
entirely by the rare earths (R', R'', etc.) in the above formula. We will
therefore identify compositions primarily by the rare earths they contain.
We will consider that all films with the same rare earth content are
basically the same composition, even if x is not the same in all samples.
This is not to say that x has no effect on some important bubble properties.
The $4\pi M$ depends directly on x and changes[7] by about 150.G for a change of
0.1 in x . Therefore, variations in x will change both ℓ and q , since
these quantities depend on $4\pi M$. Since K_u and A do not vary appreciably
for modest changes in $4\pi M$, ℓ and q vary predictably with $4\pi M$ according
to the relation

$$\ell \propto q \propto \frac{1}{M^2} \tag{3}$$

which follows directly from Eqs. (1) and (2).

In practice, LPE garnets are prepared by growing test films and
making small additions to the melt until x has the value which gives a

14

desired bubble diameter. By making such melt additions, we have grown a
series of films with a range of different bubble diameters for each basic
composition that we chose to study. To present here the data on all these
samples of each R', R'' .... combination would take a great deal of space and
would merely serve to obscure rather than clarify the significant conclusions
that can be drawn from our experiments. Instead, we present in Table I just
one set of data for each rare earth combination. Even though we are thus
compressing a large amount of experimental data into a relatively few
numbers, we still retain (as will be demonstrated below) all the essential
information on the static bubble properties of each composition. Thus the
experimental data on individual samples can be relegated to appendices I
and II without losing any information needed for a general discussion of the
relative merits of the different compositions we have prepared.

Except for one composition, the data in Table I represents a summary
of results on several films. Thus the values shown for K_u indicate the
range of values obtained upon measuring several samples. It will be seen
that these ranges are relatively small since, as mentioned above, K_u is
expected to be the same for all compositions containing the same rare earths
R', R'' .... . Unlike K_u, the parameters $4\pi M$ and q depend directly
on x . Therefore, in order to present the data in a form that can readily
be interpreted, it is necessary to separate the dependence on x from dif-
ferences which are due to the rare earth content R', R'' .... . We have
chosen to accomplish this by normalizing all data to the same ℓ value.
Thus, although we have made measurements on samples with ℓ between 0.1 and
0.7 μm, we have used Eqs. (1) and (2) to calculate what $4\pi M$ and q would
have been if ℓ had been 0.15 μm in each sample. Since the average bubble
diameter of a material is slightly less than ten times its ℓ value, the values
of $4\pi M$ and ℓ presented in Table I are therefore the values that would be
obtained in a material supporting bubbles of about 1.5 μm diameter. If one
wishes to know what $4\pi M$ would correspond to some different ℓ , the value
can easily be calculated from the simple relation

15

$$4\pi M \bigg|_{\ell} = \left[4\pi M \bigg|_{\ell\ =\ 0.15}\right]\left(\frac{0.15}{\ell}\right)^{\frac{1}{2}}$$

which follows directly from Eq. (1). Similarly, the value of q in the table is that value which corresponds to $\ell = 0.15$. To obtain the value of q for some ℓ other than 0.15, one has merely to apply the relation

$$q \bigg|_{\ell} = \left[q \bigg|_{\ell\ =\ 0.15}\right] \frac{\ell}{0.15}$$

which follows directly from Eq. (2).

A wide spectrum of materials is represented in Table I. Included are several new compositions, as well as some 6 μm bubble materials appropriately modified for small-bubble applications. As may be seen from the table, most of these materials do not fulfill the $q \geq 3$ Air Force requirement when the bubble size is ~ 1.5 μm. Those with $q < 3$ include several compositions which have been often mentioned as potential small bubble materials. Fortunately, however, there are five compositions in this table which can meet the $q \geq 3$ requirement. One of these materials (the $(YEu)_3 (FeGa)_5 O_{12}$) can be eliminated from consideration because it has a positive magnetostriction coefficient that prevents hard bubble suppression by ion implantation. Table I indicates that the remaining four high-q materials have almost ideal room-temperature static properties.

The temperature dependence of collapse field and stripe width in these four materials[*] are shown in Figs. 1 through 3. Over the -55°C to $+125^\circ$C range, the percentage changes (referred to room temperature) of stripe

---

[*]Actually, we measured the temperature dependence of only three of these four compositions. Since Table I shows $(EuTm)_3 (FeGa)_5 O_{12}$ and $(LaEuTm)_3 (FeGa)_5 O_{12}$ to have similar room temperature properties, we have assumed that their temperature dependences will also be similar and have only measured the $(LaEuTm)_3 (FeGa)_5 O_{12}$.

width and collapse field for these three materials are:

Composition	Stripe Width	Collapse Field
$(LaEuTm)_3(FeGa)_5\,O_{12}$	17.%	13.%
$(SmTm)_3(FeGa)_5\,O_{12}$	11.%	24.%
$(TbTm)_3(FeGa)_5\,O_{12}$	102.%	47.%

Clearly, the $(TbTm)_3(FeGa)_5\,O_{12}$ has a poor temperature dependence, but the other two materials are very good. As a matter of fact, it would be hard to conceive of appreciably less variation being achieved in any bubble garnet. Thus, we have two materials, $(SmTm)_3(FeGa)_5\,O_{12}$ and $(LaEuTm)_3(FeGa)_5\,O_{12}$ with almost ideal static bubble properties. Obviously, our next task is to evaluate their dynamic properties.

TABLE I

BASIC STATIC BUBBLE DATA FOR
VARIOUS SMALL-BUBBLE GARNETS

Composition	$10^4 K_u$ (ergs/cm^3)	for $\ell = 0.15\ \mu m$	
		q	$4\pi M$ (G)
$(YLaTm)_3(FeGa)_5\ O_{12}$[4]	0.9-2.0	1.4-1.7	370.-590.
$(YEuLuCa)_3(FeGe)_5\ O_{12}$[3,4]	0.4-2.6	0.5-1.7	290.-810.
$(YSmLuCa)_3(FeGe)_5\ O_{12}$[4]	0.5-1.1	1.2-1.7	380.-480.
$(YEu)_3(FeGa)_5\ O_{12}$[1]	2.5-5.9	1.6-5.1	540.-620.
$(EuTm)_3(FeGa)_5\ O_{12}$[2]	6.7	3.9	655.
$(LaEuTm)_3(FeGa)_5\ O_{12}$[4]	5.2-7.5	2.9-5.3	520.-790.
$(SmTm)_3(FeGa)_5\ O_{12}$	12.2	3.9-6.9	670.-880.
$(TbTm)_3(FeGa)_5\ O_{12}$	9.7-13.0	3.4-5.7	650.-970.
$(LaTm)_3(FeGa)_5\ O_{12}$	0.3	0.7-1.8	330.-540.

1. This composition was grown on a (110) $Sm_3Ga_5O_{12}$ substrate and was mismatched to this substrate so that the anisotropy was primarily strain induced. All other samples were grown on [111] $Gd_3Ga_5\ O_{12}$ and were closely matched to the substrate (to within .003Å).

2. Only one sample was measured of this composition. Several samples were prepared of each of the other materials; in cases where not all samples gave the same results, the range of values is indicated. Representative experimental data from which this table was derived may be found in Appendix I.

3. The wide range of observed values for this material may be due to inhomogeneities such as have been reported[8] in other garnets containing Ca or Ge.

18

4. In garnet films with only two rare earths, there is a unique concen-
   tration of each that will permit the film to match the substrate.
   However, in materials having three rare earths, there is a range of
   relative concentrations which yield a match. Therefore, although we
   believe the results given here are typical, there may be other formu-
   lations of these compositions yielding somewhat different results.
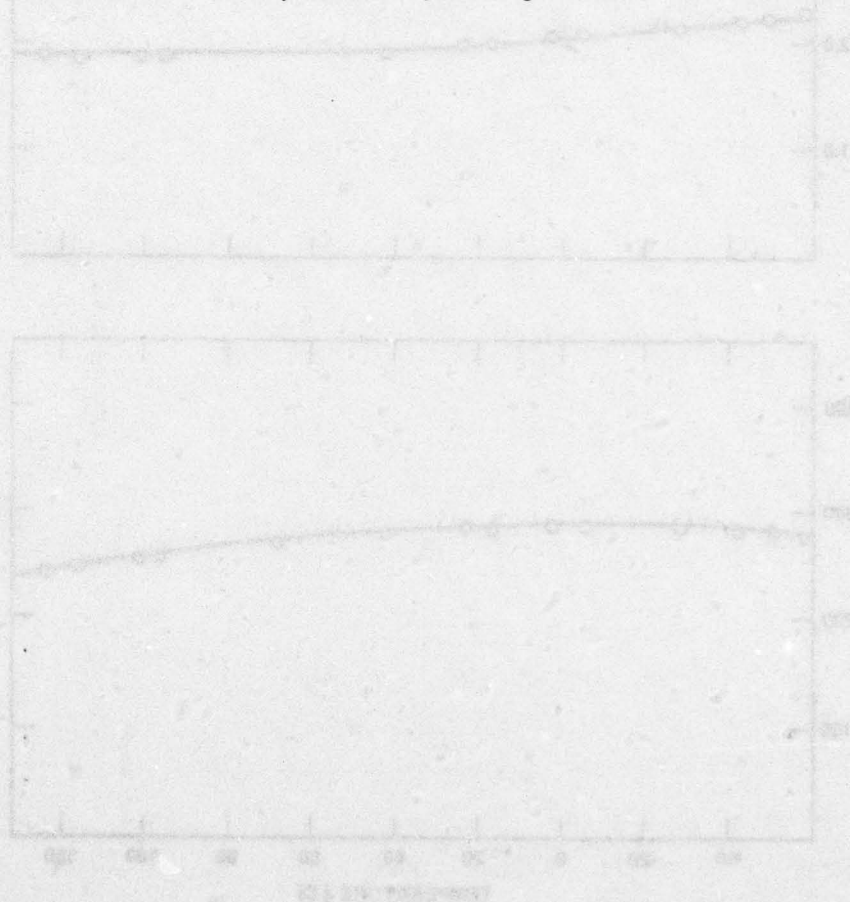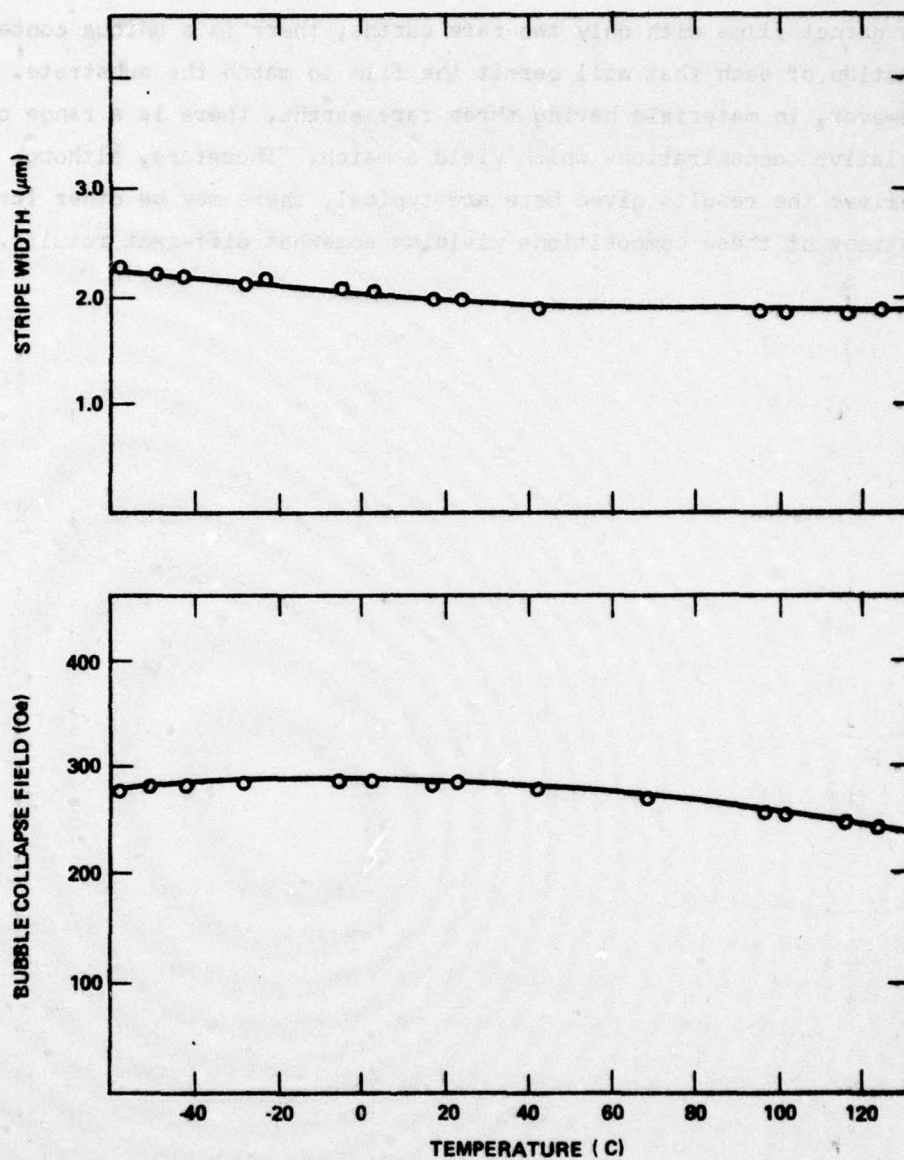
FIG. 1   Stripe width and bubble collapse field for $(LaEuTm)_3(FeGa)_5O_{12}$
as a function of temperature.
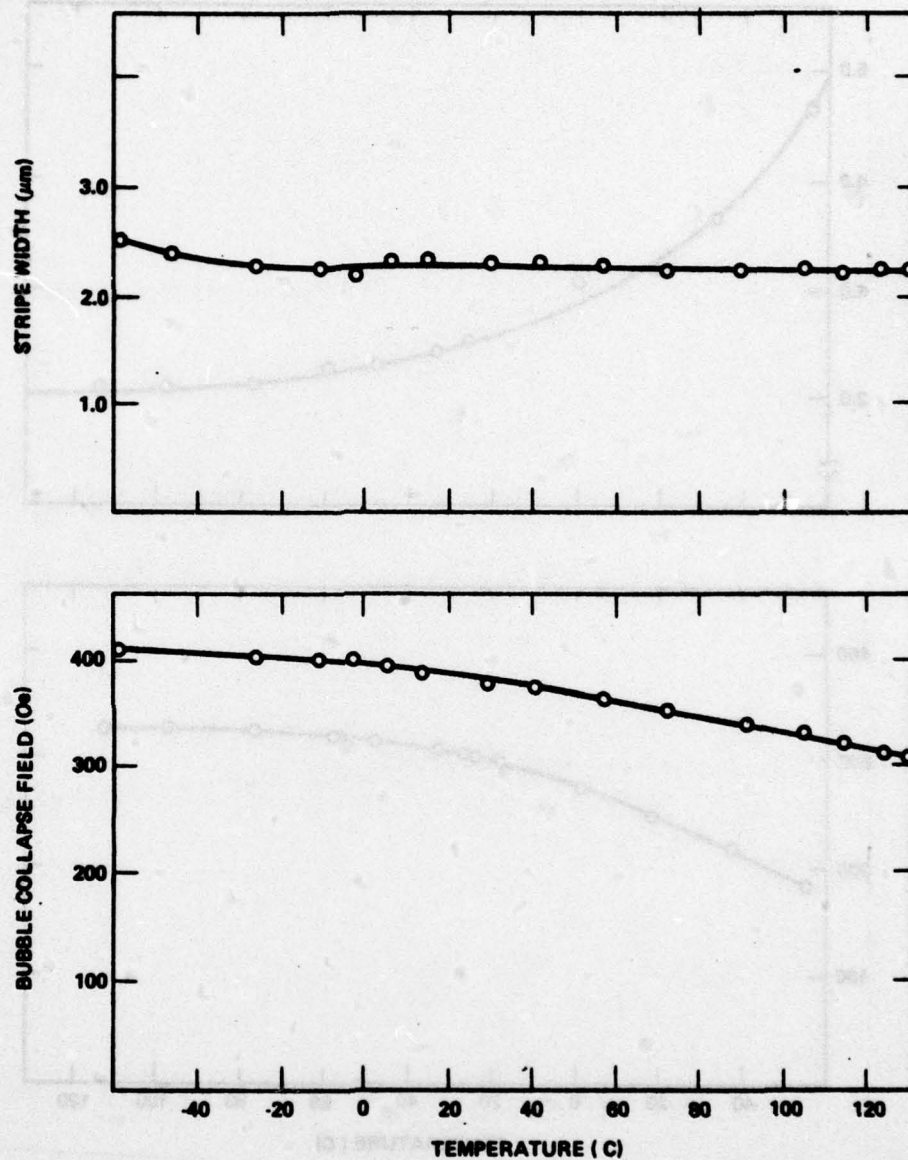
FIG. 2   Stripe width and bubble collapse field for $(SmTm)_3 (FeGa)_5 O_{12}$
as a function of temperature.
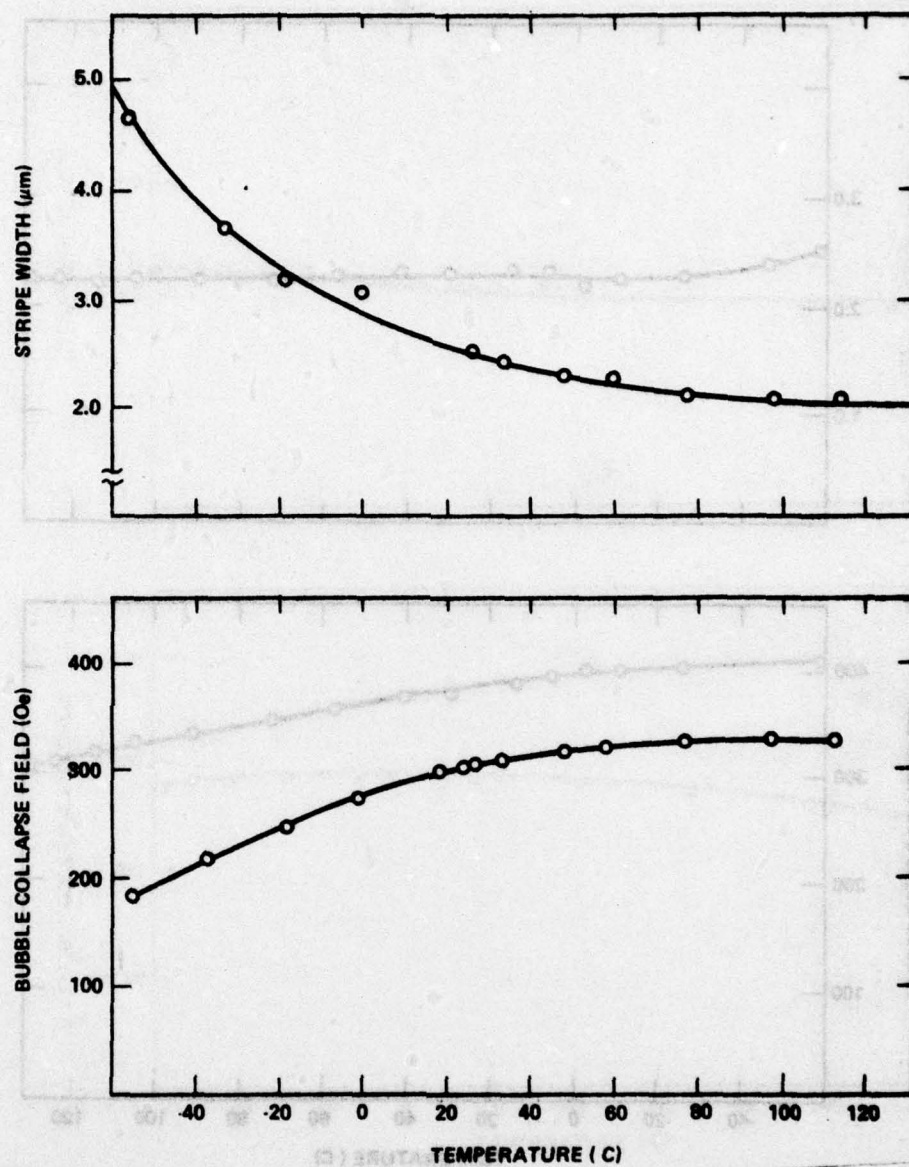
FIG. 3   Stripe width and bubble collapse field for $(TbTm)_3(FeGa)_5O_{12}$ as a function of temperature.

22

SECTION VIII

PLANS FOR THE NEXT REPORT PERIOD

In the course of our measurements, we have found two compositions which show good static small-bubble properties and also have relatively temperature-independent collapse fields and stripe widths. Thus all the known properties of these materials are very favorable for small-bubble applications. However, a number of important properties still remain to be checked in these materials.

In the near future, we plan to make bubble-shift velocity measurements which will yield mobility, coercivity, and saturation velocity data on these materials. In addition to this dynamic data, two further temperature-dependence studies should be made. We shall measure the temperature dependence of the anisotropy field to verify that q does not drop below 3 at temperatures up to 125°C. Also, we will determine the Curie point by microscopic observation using the Hsu-Bellavance technique. In addition to the above studies, we must also devise a successful method of hard bubble suppression for each composition in order for it to be useful in device applications. As a matter of fact, hard bubble suppression may have to be achieved in a given composition before a complete and meaningful set of velocity data can be obtained.

The results of all the above described measurements will almost certainly point to the need for compositional changes, or perhaps to the necessity for developing new compositions. We will prepare new films as the need for them arises and then make the appropriate magnetic measurements.

23

APPENDIX A

TABULATION OF REPRESENTATIVE SMALL
BUBBLE DIAMETER EXPERIMENTAL RESULTS

In Table I we gave a summary of the experimental data taken on a large number of films. The purpose of this appendix is to present (by means of Table II) a representative sample of the experimental data on which Table I was based. This data in Table II includes film thickness, zero-field stripe width, $4\pi M$, ℓ, K_u and q. The table also contains the normalized q and $4\pi M$ values which are discussed in connection with Table I.

TABLE II

TABULATION OF REPRESENTATIVE SMALL BUBBLE DIAMETER EXPERIMENTAL RESULTS

MATERIAL	SAMPLE NUMBER	FILM THICKNESS (μm)	ZERO FIELD STRIPE WIDTH (μm)	$4\pi M$ (G)	ℓ (μM)	$10^{-4} K_u$ (ergs/cm^3)	q	NORMALIZED TO $\ell = 0.15$ μm q	$4\pi M$ (G)
$(YLaTm)_3(FeGa)_5 O_{12}$ [4]	50418B	6.4	3.3	350.	0.228	1.21	2.48	1.63	429.
	50417B	6.6	2.5	402.	0.128	0.917	1.43	1.68	371.
	50605B	1.0	1.0	683.	0.113	~1.96	~1.1	~1.5	593.
	50516C	2.0	1.0	693.	0.067	1.20	0.63	~1.41	463.
$(YEuLaCa)_3(FeGe)_5 O_{12}$ [3,4]	60329B	4.3	2.2	539.	0.151	2.01	1.75	1.74	541.
	60406B	3.8	2.1	802.	0.154	2.58	1.01	0.98	813.
	60615A	6.0	3.9	194.	0.329	0.394	2.63	1.20	287.
	60616D	3.8	3.0	355.	0.293	0.5	1.0	0.51	496.
$(YSmLuCa)_3(FeGe)_5 O_{12}$ [4]	60922C	2.2	2.2	296.	0.248	0.47	2.8	1.70	380.
	60923B	1.7	2.0	376.	0.242	1.10	1.9	1.18	477.
	60923D	2.1	2.0	325.	0.219	0.89	2.1	1.44	392.
$(YEu)_3(FeGa)_5 O_{12}$ [1]	41112A	4.43	1.95	559.	0.140	5.93	4.76	5.10	540.
	41105B	3.88	1.48	866.	0.076	2.49	0.83	1.64	617.
$(EuTm)_3(FeGa)_5 O_{12}$ [4]	50625A	3.3	3.0	470.	0.291	6.7	7.64	3.94	655.
$(LaEuTm)_3(FeGa)_5 O_{12}$ [4]	60707A	1.0	2.2	483.	0.292	5.2	5.6	2.87	674.
	60708B	2.1	2.4	484.	0.298	5.8	6.2	3.12	683.
	60716B	2.5	1.7	526.	0.149	5.9	5.3	5.3	523.
	60715C	1.8	1.9	650.	0.220	7.5	4.5	3.06	788.
$(SmTm)_3(FeGa)_5 O_{12}$	61019A	3.6	2.1	645.	0.161	12.2	7.4	6.9	667.
	61019B	3.6	3.4	561.	0.372	12.2	9.7	3.9	889.
$(TbTm)_3(FeGa)_5 O_{12}$	61204A	7.8	6.7	304.	0.694	9.7	26.3	5.7	654.
	61204B	3.1	5.5	441.	0.729	13.0	16.4	3.4	972.
$(LaTm)_3(FeGa)_5 O_{12}$	61014D	3.5	1.7	633.	0.110	0.86	0.54	0.74	541.
	61027D	5.8	4.7	188.	0.467	0.77	5.5	1.77	332.

26

APPENDIX B

TABULATION OF MAGNETIC DATA FOR
SAMPLES DELIVERED TO CONTRACT MONITOR

Once a month since the beginning of this contract, we have sent representative garnet films to WPAFB. The purpose of this appendix is to summarize the properties of these films. In Table III, we have listed the composition, film thickness, and magnetic properties for all of these films.

TABLE III

TABULATION OF MAGNETIC DATA FOR SAMPLES DELIVERED TO CONTRACT MONITOR

Date of Shipment to WPAFB	SAMPLE NUMBER	SAMPLE COMPOSITION	FILM THICKNESS (μm)	ZERO-FIELD STRIPE WIDTH (μm)	$4\pi M$ (G)	ℓ (μm)	$10^{-4}K_u$ (ergs/cm^3)	q
7/20/76	1	$(LaEuTm)_3(FeGa)_5 O_{12}$	2.7	1.9	526.	0.171	5.9	5.3
	2	"	1.9	1.8	591.	0.197	6.8	4.9
	3	"	2.2	1.8	516.	0.180	5.7	5.4
	4	"	1.8	1.9	650.	0.220	7.5	4.5
8/2/76	5	$(YLaTm)_3(FeGa)_5 O_{12}$	1.8	1.2	688.	0.100	1.6	0.6
	6	" (implanted)	2.9	1.5	551.	0.104	1.4	0.9
	7	" (implanted)	4.0	1.9	488.	0.121	1.2	1.1
	8	"	1.5	1.0	590.	0.086	1.3	0.7
	9	G^3 SUBSTRATE						
8/27/76	1	$(LaEuTm)_3(FeGa)_5 O_{12}$	2.1	2.0	489.	0.219	6.2	6.5
	2	"	2.3	2.0	504.	0.208	6.4	6.3
	3	"	1.6	2.0	559.	0.247	7.1	5.7
	4	G^3 SUBSTRATE						
	5	$(LaEuTm)_3(FeGa)_5 O_{12}$	1.5	1.9	512.	0.236	7.5	7.2
	6,7,8	"	3.6	2.6	533.	0.238	6.6	5.8
9/29/76	1	$(YSmLuCa)_3(FeGe)_5 O_{12}$	2.2	2.2	296.	0.248	0.97	2.8
	2	"	2.3	2.2	291.	0.241	0.87	2.6
	3	"	2.1	2.0	325.	0.219	0.89	2.1
	4	"	1.9	2.0	289.	0.231	0.75	2.2
	5	G^3 SUBSTRATE						
10/29/76	5-1	G^3 SUBSTRATE						
	5-2	$(LaEuTm)_3(FeGa)_5 O_{12}$	1.6	1.9	563.	0.231	7.4	5.9
	5-3	$(EuTm)_3(FeGa)_5 O_{12}$	2.0	2.3	———— not measured ————			
	5-4	$(SmTm)_3(FeGa)_5 O_{12}$	3.6	2.1	645.	0.161	12.2	7.4
	5-5	$(YSmLuCa)_3(FeGe)_5 O_{12}$	1.7	2.0	376.	0.242	1.1	1.9
12/3/76	1	$(LaEuTm)_3(FeGa)_5 O_{12}$	2.7	2.0	588.	0.186	6.8	4.9
	2	$(TbTm)_3(FeGa)_5 O_{12}$	2.6	2.8	———— not measured ————			
	3	"	3.1	2.5	———— not measured ————			
	4	"	2.1	2.2	———— not measured ————			
	5	G^3 SUBSTRATE						
12/15/76	1	$(TbTm)_3(FeGa)_5 O_{12}$	1.9	1.4	———— not measured ————			
	2	"	2.0	1.7	———— not measured ————			
	3	"	1.6	1.9	———— not measured ————			
	4	G^3 SUBSTRATE						

REFERENCES

1. D. C. Fowlis and J. A. Copeland, AIP Conf. Proc. $\underline{5}$, 240 (1971).

2. R. M. Josephs, AIP Conf. Proc. $\underline{10}$, 286 (1972).

3. A. J. Kurtzig and F. B. Hagedorn, IEEE Trans. $\underline{MAG-7}$, 473 (1971).

4. A. B. Smith, M. Kestigian and W. R. Bekebrede, AIP Conf. Proc. $\underline{10}$, 309 (1972).

5. W. T. Stacy, M. M. Janssen, J. M. Robertson and M. J. G. VanHout, AIP Conf. Proc. $\underline{10}$, 314 (1972).

6. W. F. Druyvesteyn, J. W. F. Dorleijn and P. J. Rijnierse, J. Appl. Phys. $\underline{44}$, 2397 (1973).

7. W. H. VonAulock, "Handbook of Microwave Ferrite Materials," Academic Press, New York, 1965, p 114.

8. M. Kestigian, A. B. Smith and W. R. Bekebrede, Mat. Res. Bull. $\underline{11}$, 773 (1976).